

# Using Higgs Pair Production in $e^+e^-$ or $\mu^+\mu^-$ Collisions To Probe GUT-Scale Boundary Conditions in the Minimal Supersymmetric Model\*

J. F. Gunion and J. Kelly<sup>†</sup>*Davis Institute for High Energy Physics, University of California, Davis, California 95616*

## ABSTRACT

We delineate the techniques and prospects for using Higgs pair production in  $e^+e^-$  or  $\mu^+\mu^-$  collisions to probe GUT-scale boundary conditions in the minimal supersymmetric standard model.

## I. Introduction and Results

The heavier CP-even, the CP-odd and the charged Higgs bosons ( $H^0$ ,  $A^0$ , and  $H^\pm$ , respectively) of the minimal supersymmetric standard model (MSSM) (see Ref. [1] for a recent review) are typically predicted to be fairly heavy (with  $m_{H^0} \sim m_{A^0} \sim m_{H^\pm} \gtrsim 200$  GeV) in models where electroweak symmetry breaking at scale  $m_Z$  arises as a result of evolution beginning from simple GUT/Planck-scale boundary conditions. Nonetheless, once  $\sqrt{s}$  is large enough that  $e^+e^- \rightarrow H^0 A^0$  and  $e^+e^- \rightarrow H^+ H^-$  (or their  $\mu^+\mu^-$  analogues) are kinematically possible, event rates are substantial for expected machine luminosities, and discovery and study of these Higgs bosons becomes possible [2]. The all-jet and high-multiplicity final states coming from  $H^0, A^0 \rightarrow b\bar{b}, t\bar{t}$  and  $H^\pm \rightarrow t\bar{b}, H^- \rightarrow b\bar{t}$  are background free and for the model we study provide appropriate and efficient signals with rates that are adequate even when SUSY decays are present. Further, in the all-jet channels, the individual Higgs boson masses,  $m_{A^0}$ ,  $m_{H^0}$  and  $m_{H^\pm}$ , can be measured. Event rates and decay branching fractions are typically such that it will be possible to ‘tag’ one member the pair in such a fully reconstructable final state and then study the decays of the untagged member of the pair. Here, we point out the very dramatic sensitivity of measurements of decay branching fractions to the GUT boundary condition scenario, illustrating in particular the high statistical level at which various not terribly different scenarios can be distinguished from one another using ratios of branching fractions. A more detailed treatment of this analysis appears in Ref. [2].

In the simplest GUT treatments of the MSSM, soft supersymmetry breaking at the GUT scale is specified by three universal parameters:

- $m_0$ : the universal soft scalar mass;
- $m_{1/2}$ : the universal soft gaugino mass;
- $A_0$ : the universal soft Yukawa coefficient.

The absolute value of  $\mu$  (the Higgs mixing parameter) is determined by requiring that radiative EWSB gives the exact value of  $m_Z$  for the experimentally measured value of  $m_t$ ; however, the sign of  $\mu$  remains undetermined. Thus, the remaining parameters required to completely fix the model are

- $\tan \beta$ : the vacuum expectation value ratio; and
- $\text{sign}(\mu)$ .

We remind the reader that a universal gaugino mass at the GUT scale implies that  $M_3 : M_2 : M_1 \sim 3 : 1 : 1/2$  at scale  $\sim m_Z$ . For models of this class one also finds that  $\mu \gg M_{1,2}$ . These two facts imply that the  $\tilde{\chi}_1^0$  is mainly bino, while  $\tilde{\chi}_2^0$  and  $\tilde{\chi}_1^\pm$  are mainly wino, with heavier gauginos being mainly higgsino, so that  $m_{\tilde{\chi}_2^0} \sim m_{\tilde{\chi}_1^\pm} \sim 2m_{\tilde{\chi}_1^0}$ .

We will consider three representative GUT scenarios characterized by increasingly large values of  $m_0$  relative to  $m_{1/2}$  (which translates into increasingly large slepton masses as compared to  $m_{\tilde{\chi}_1^0}$ ,  $m_{\tilde{\chi}_2^0}$ , and  $m_{\tilde{\chi}_1^\pm}$ ):

- “No-Scale” (NS):  $A_0 = m_0 = 0$ ;
- “Dilaton” (D):  $m_{1/2} = -A_0 = \sqrt{3}m_0$ ;
- “Heavy-Scalar” (HS):  $m_0 = m_{1/2}$ ,  $A_0 = 0$ .

Within any one of these three scenarios, the model is completely specified by values for  $m_{1/2}$ ,  $\tan \beta$  and  $\text{sign}(\mu)$ . We will present results in the  $(m_{1/2}, \tan \beta)$  parameter space for a given  $\text{sign}(\mu)$  and a given choice of scenario. Our notation will be  $NS^-$  for the no-scale scenario with  $\text{sign}(\mu) < 0$ , and so forth.

In exploring each of these scenarios, we proceed as follows.

- First, we delineate the allowed region of  $(m_{1/2}, \tan \beta)$  parameter space consistent with all available experimental and phenomenological constraints (such as the LSP being uncharged, coupling constants remaining perturbative, no Higgs or SUSY particle having been observed at LEP, *etc.*). The extent of these regions is quite limited for the NS models, and is largest for the HS models.
- Second, we determine the masses of the Higgs bosons and SUSY particles as a function of  $(m_{1/2}, \tan \beta)$ . The masses of the inos and the sleptons will presumably be measured quite accurately, and they will determine the values of  $m_{1/2}$  and  $m_0$ ; but  $\tan \beta$  is likely to be poorly determined from these masses alone. However, a measurement of  $m_{A^0}$  (or  $m_{H^0}$  or  $m_{H^\pm}$ ) in combination with the  $m_{1/2}$  determination from the ino masses will fix a value of  $\tan \beta$ . The accuracy of this determination depends upon the accuracy

\* To appear in “Proceedings of the 1996 DPF/DPB Summer Study on New Directions for High Energy Physics”. Work supported in part by the Department of Energy and in part by the Davis Institute for High Energy Physics.

<sup>†</sup> Current address: Dept. of Physics, University of Wisconsin, Wisconsin, Madison WI 53706.

with which  $m_{A^0}$  (and  $m_{H^0}$ ,  $m_{H^\pm}$ ) can be measured. For the  $A^0, H^0 \rightarrow b\bar{b}$  decay modes, for example, this accuracy is fixed by the  $b\bar{b}$  mass resolution. A resolution of  $\pm\Delta M_{bb} \sim \pm 10$  GeV is probably attainable. For a large number,  $N$ , of events,  $m_{A^0}$  can be fixed to a value of order  $\Delta M_{bb}/\sqrt{N}$ , which for  $N = 20$  (our minimal discovery criterion) would imply  $\Delta m_{A^0} \sim 2 - 3$  GeV. Such mass uncertainty will lead to a rather precise  $\tan\beta$  determination within a given GUT model (except in special cases).

- Finally, we examine the Higgs branching ratios as a function of location in  $(m_{1/2}, \tan\beta)$  parameter space, and determine the statistical accuracy with which these branching ratios can be measured for reasonable assumptions regarding Higgs tagging and reconstruction efficiencies.

Ratios of branching ratios are of particular interest since certain types of systematic errors will cancel. Relative Higgs branching ratios can be measured by ‘tagging’ one member of the produced pair using a fully reconstructable all-jet decay mode, and then looking at the various final states emerging from the decay of the other member of the pair. Using the measured values of  $B(h^0 \rightarrow b\bar{b})$  and  $B(t \rightarrow 2jb)$  and with experimental knowledge of efficiencies, we can thus measure

$$\frac{B(H^0 \rightarrow \text{SUSY})B_{\text{eff}}(A^0 \rightarrow b\bar{b} + t\bar{t}) + B(A^0 \rightarrow \text{SUSY})B_{\text{eff}}(H^0 \rightarrow b\bar{b} + t\bar{t})}{B_{\text{eff}}(H^0 \rightarrow b\bar{b} + t\bar{t})B_{\text{eff}}(A^0 \rightarrow b\bar{b} + t\bar{t})} \quad (1)$$

$$\frac{B(H^0 \rightarrow t\bar{t})B(A^0 \rightarrow b\bar{b}) + B(A^0 \rightarrow t\bar{t})B(H^0 \rightarrow b\bar{b})}{B(H^0 \rightarrow b\bar{b})B(A^0 \rightarrow b\bar{b})} \quad (2)$$

$$\frac{B(H^0 \rightarrow h^0 h^0)B(A^0 \rightarrow b\bar{b})}{B(H^0 \rightarrow b\bar{b})B(A^0 \rightarrow b\bar{b})} \quad (3)$$

$$\frac{B(A^0 \rightarrow Zh^0)B(H^0 \rightarrow b\bar{b})}{B(H^0 \rightarrow b\bar{b})B(A^0 \rightarrow b\bar{b})} \quad (4)$$

$$\frac{B(H^+ \rightarrow \text{SUSY})B(H^- \rightarrow b\bar{t}) + B(H^- \rightarrow \text{SUSY})B(H^+ \rightarrow t\bar{b})}{B(H^+ \rightarrow t\bar{b})B(H^- \rightarrow b\bar{t})} \quad (5)$$

$$\frac{B(H^+ \rightarrow \tau^+ \nu)B(H^- \rightarrow b\bar{t}) + B(H^- \rightarrow \tau^- \nu)B(H^+ \rightarrow t\bar{b})}{B(H^+ \rightarrow t\bar{b})B(H^- \rightarrow b\bar{t})} \quad (6)$$

$$\frac{B(H^+ \rightarrow h^0 W^+)B(H^- \rightarrow b\bar{t}) + B(H^- \rightarrow h^0 W^-)B(H^+ \rightarrow t\bar{b})}{B(H^+ \rightarrow t\bar{b})B(H^- \rightarrow b\bar{t})} \quad (7)$$

The SUSY final states can be identified by the presence of missing energy opposite the fully reconstructable all jet mode(s) used to tag the first member of the Higgs pair. We retain both  $b\bar{b}$  and  $t\bar{t}$  final states in Eq. (1), using an efficiency weighted combination denoted by  $B_{\text{eff}}$ , in order that we may assess the importance of SUSY decays both in regions where  $b\bar{b}$  decays of the  $H^0, A^0$  are dominant and in regions where  $t\bar{t}$  decays are important. Note that since  $m_{A^0} \sim m_{H^0}$  we cannot separate the  $H^0$  and  $A^0$  decays to the same final state; we can only measure the indicated ‘average’ values of Eqs. (1) and (2).

Two illustrations are provided. In Figs. 1 and 2 we show contours in  $(m_{1/2}, \tan\beta)$  parameter space of constant values for the ratio of Eqs. (1) and (5), respectively, for each of the six scenarios defined earlier. The three different curves for each value of the ratio indicate the precision with which experiment can determine a location in parameter space. These results are based on event rates calculated including all relevant branching ratios and assuming an ‘effective’ integrated luminosity of  $L_{\text{eff}} = 80 \text{ fb}^{-1}$  at  $\sqrt{s} = 1$  TeV, where  $L_{\text{eff}} = 80 \text{ fb}^{-1}$  includes an overall tagging, detection, and so forth, efficiency of  $\epsilon = 0.2$

at  $L = 400 \text{ fb}^{-1}$  (about two years of running). We observe that the precision is actually rather good. Since the  $H^0 A^0$  and  $H^+ H^-$  SUSY ratio contours displayed tend to cross one another, a measurement of these two ratios will determine a location in  $(m_{1/2}, \tan\beta)$  parameter space in each GUT scenario. It turns out that this determination in one model often disagrees at a statistically very significant level with the location determined on the basis of the  $m_{\tilde{\chi}_1^\pm}$  and  $m_{A^0}$  masses, described earlier, for any other model.

$$2 < B(H^0, A^0 \rightarrow \text{SUSY}) / B_{\text{eff}}(H^0, A^0 \rightarrow b\bar{b} \text{ or } t\bar{t}) >$$

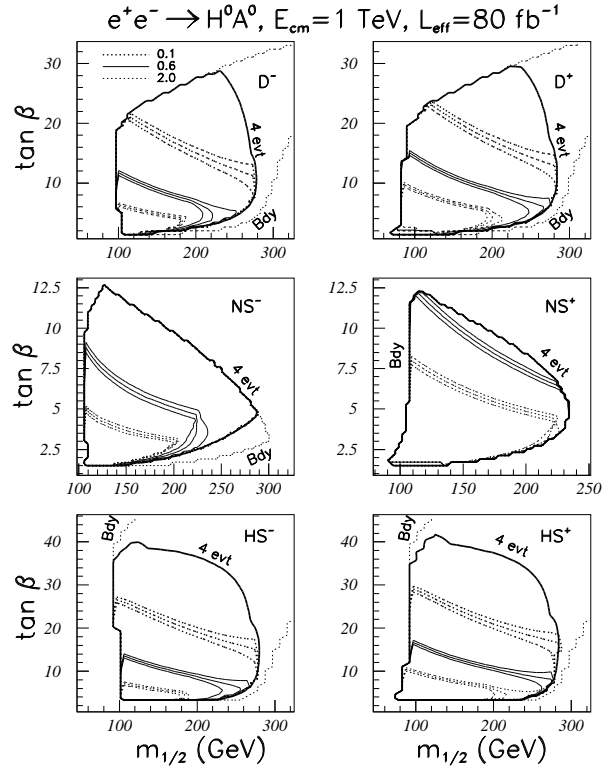


Figure 1: We plot contours along which the ratio of Eq. (1) has a given constant value, within the constraint/kinematically allowed  $(m_{1/2}, \tan\beta)$  parameter space (as indicated by the ‘Bdy’ lines) of the  $D^-, D^+, NS^-, NS^+, HS^-,$  and  $HS^+$  models. Results are shown for the same three central values for all models. For each central value, three lines are drawn. The central line is for the central value. The other two lines are contours for which the ratio deviates by  $\pm 1\sigma$  statistical error (see Ref. [2]) from the central value. Bold lines indicate the boundary beyond which fewer than 4 events are found in the final states used to measure the numerator of the ratio.

To more thoroughly illustrate the extent to which the set of ratios given in Eqs. (1)-(7) can distinguish between scenarios, let us focus on one particular case. Suppose the correct model

$$2 \cdot B(H^+ \rightarrow \text{SUSY}) / B(H^+ \rightarrow tb)$$

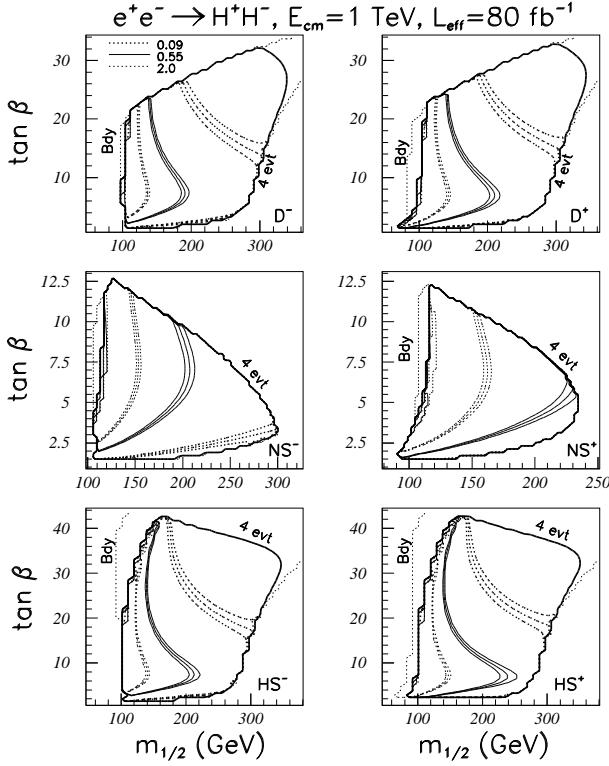


Figure 2: As in Fig. 1, but for the ratio of Eq. (5).

is  $D^-$  with  $m_{1/2} = 201.7$  GeV and  $\tan \beta = 7.50$ . This would imply  $m_{A^0} = 349.7$  GeV,  $m_{\tilde{\chi}_1^\pm} = 149.5$  GeV. The  $m_{1/2}$  and  $\tan \beta$  values required in order to reproduce these same  $m_{A^0}$  and  $m_{\tilde{\chi}_1^\pm}$  values in the other scenarios are listed in Table I. Also given in this table are the predicted values of  $m_{H^0}$  and  $m_{\tilde{\ell}_R}$  for each scenario. In order to get a first feeling for event numbers and for the errors that might be expected for the ratios of interest, we give in Table II the numbers of events,  $\mathcal{N}$  and  $\mathcal{D}$ , predicted in each scenario for use in determining the numerators and denominators of Eqs. (1)-(4) and Eqs. (5)-(7), assuming  $L_{\text{eff}} = 80 \text{ fb}^{-1}$  at  $\sqrt{s} = 1$  TeV. These numbers include the SUSY branching fractions,  $B_{\text{eff}}$ , and so forth.

In Table III we quantify the process of excluding the  $D^+$ ,  $NS^-$ ,  $NS^+$ ,  $HS^-$ , and  $HS^+$  scenarios relative to the input  $D^-$  scenario. There we give the contribution to  $\Delta\chi^2$  (computed relative to the assumed-to-be-correct  $D^-$  scenario) for each of a selection of independently measurable ratios. Also given for each of the incorrect scenarios is the sum of these contributions. This table shows that the  $D^-$  scenario can be distinguished from the  $D^+$ ,  $NS^-$ ,  $NS^+$ , and  $HS^+$  scenarios at an extremely high statistical level. Further, even though no one of the branching frac-

Table I: We tabulate the values of  $m_{1/2}$  (in GeV) and  $\tan \beta$  required in each of our six scenarios in order that  $m_{A^0} = 349.7$  GeV and  $m_{\tilde{\chi}_1^\pm} = 149.5$  GeV. Also given are the corresponding values of  $m_{H^0}$  and  $m_{\tilde{\ell}_R}$ . Masses are in GeV.

	$D^-$	$D^+$	$NS^-$	$NS^+$	$HS^-$	$HS^+$
$m_{1/2}$	201.7	174.4	210.6	168.2	203.9	180.0
$\tan \beta$	7.50	2.94	3.24	2.04	12.06	3.83
$m_{H^0}$	350.3	355.8	353.9	359.0	350.1	353.2
$m_{\tilde{\ell}_R}$	146.7	127.5	91.0	73.9	222.9	197.4

Table II: We give the numbers of events predicted in each scenario at the parameter space locations specified in Table I available for determining the numerators and denominators of Eqs. (1)-(4) and Eqs. (5)-(7). These event rates are those for  $L_{\text{eff}} = 80 \text{ fb}^{-1}$  at  $\sqrt{s} = 1$  TeV. They include all branching fractions. Our notation is  $\mathcal{N}_{(\#)}$  and  $\mathcal{D}_{(\#)}$  for the event rates in the numerator and denominator, respectively, of the ratio defined in Eq. (#).

	$D^-$	$D^+$	$NS^-$	$NS^+$	$HS^-$	$HS^+$
$\mathcal{N}_{(1)}$	97.0	92.3	88.3	49.2	76.1	124.0
$\mathcal{N}_{(2)}$	0.1	0.7	3.8	1.02	0.0	0.2
$\mathcal{N}_{(3)}$	16.4	2.7	46.6	1.47	3.8	2.4
$\mathcal{N}_{(4)}$	2.0	1.3	9.2	0.6	0.4	1.1
$\mathcal{D}_{(1)}$	198	9.6	62.1	2.6	250	18.2
$\mathcal{D}_{(2)-(4)}$	198	8.9	58.3	1.6	250	18.0
$\mathcal{N}_{(5)}$	225	189	138	135	189	262
$\mathcal{N}_{(6)}$	58.4	4.2	6.5	1.1	90.0	9.5
$\mathcal{N}_{(7)}$	13.0	12.8	21.9	9.0	3.3	12.3
$\mathcal{D}_{(5)-(7)}$	317	415	445	465	320	348

tion ratios provides an absolutely clear discrimination between the  $D^-$  and the  $HS^-$  scenarios, the accumulated discrimination power obtained by considering all the ratios is very substantial. In particular, although the ratios of Eq. (3), (4), and (7) are only poorly measured for  $L_{\text{eff}} = 80 \text{ fb}^{-1}$ , their accumulated  $\Delta\chi^2$  weight can be an important component in determining the likelihood of a given model and thereby ruling out incorrect model choices.

Thus, consistency of all the ratios with one another and with the measured  $m_{A^0}$ , neutralino and chargino masses will generally restrict the allowed models to ones that are very closely related. The likelihood or probability associated with the best fit to all these observables in a model that differs significantly from the correct model would be very small.

An important issue is the extent to which one can be sensitive to the branching fractions for different types of SUSY decays of the Higgs bosons, relative to one another and relative to the overall SUSY decay branching fraction. Rates in different channels depend in a rather detailed fashion upon the SUSY parameters and would provide valuable information regarding the SUSY scenario. For example, in going from NS to D to HS the

Table III: We tabulate  $\Delta\chi_i^2$  (relative to the  $D^-$  scenario) for the indicated branching fraction ratios as a function of scenario, assuming the measured  $m_{A^0}$  and  $m_{\tilde{\chi}_1^\pm}$  values are 349.7 GeV and 149.5 GeV, respectively. The SUSY channels have been resolved into final states involving a fixed number of leptons. The error used in calculating each  $\Delta\chi_i^2$  is the approximate  $1\sigma$  error with which the given ratio could be measured for  $L_{\text{eff}} = 80 \text{ fb}^{-1}$  at  $\sqrt{s} = 1 \text{ TeV}$  assuming that the  $D^-$  scenario is the correct one.

Ratio	$D^+$	$NS^-$	$NS^+$	$HS^-$	$HS^+$
$(H^0, A^0)$					
$[0\ell][\geq 0j]/bb, t\bar{t}$	12878	1277	25243	0.77	10331
$[1\ell][\geq 0j]/bb, t\bar{t}$	13081	2.41	5130	3.6	4783
$[2\ell][\geq 0j]/bb, t\bar{t}$	4543	5.12	92395	26.6	116
$h^0 h^0/b\bar{b}$	109	1130	1516	10.2	6.2
$H^\pm$					
$[0\ell][\geq 0j]/t\bar{b}$	12.2	36.5	43.2	0.04	0.2
$[1\ell][\geq 0j]/t\bar{b}$	1.5	0.3	0.1	5.6	0.06
$h^0 W/t\bar{b}$	0.8	0.5	3.6	7.3	0.3
$\tau\nu/t\bar{b}$	43.7	41.5	47.7	13.7	35.5
$\sum_i \Delta\chi_i^2$	30669	2493	124379	68	15272

masses of the sneutrinos and sleptons increase relative to those for the charginos and neutralinos. The  $H^0, A^0 \rightarrow \tilde{\ell}^+ \tilde{\ell}^-$  and  $H^\pm \rightarrow \tilde{\ell}^\pm \tilde{\nu}$  branching fractions should decline in comparison to  $H^0, A^0 \rightarrow \tilde{\chi}_1^+ \tilde{\chi}_1^-$  and  $H^\pm \rightarrow \tilde{\chi}_1^\pm \tilde{\chi}_1^0$ , respectively. In small sections of the D and NS scenario parameter spaces, the sleptons and sneutrinos are sufficiently light that  $\tilde{\chi}_1^\pm$  decays almost exclusively to  $\tilde{\ell}^\pm \tilde{\nu}$  followed by  $\tilde{\ell}^\pm \tilde{\nu} \rightarrow \ell^\pm \tilde{\chi}_1^0 \nu \tilde{\chi}_1^0$ , implying that  $\tilde{\chi}_1^\pm$  decays would mainly yield leptons and not jets.

The difficulty is that several different SUSY channels can contribute to any given final state. For example, the  $\ell^+ \ell^- + \cancel{E}_T$  channel receives contributions from both  $H^0, A^0 \rightarrow \tilde{\ell}^+ \tilde{\ell}^-$  and  $\tilde{\chi}_1^+ \tilde{\chi}_1^-$  decays; and the  $\ell^\pm + \cancel{E}_T$  channel receives contributions from  $H^\pm \rightarrow \tilde{\ell}^\pm \tilde{\nu}$  and  $\tilde{\chi}_1^\pm \tilde{\chi}_1^0$ . Another example, is the purely invisible  $H^0$  or  $A^0$  final state; it can arise from either  $\tilde{\chi}_1^0 \tilde{\chi}_1^0$  or  $\tilde{\nu} \tilde{\nu}$  (with  $\tilde{\nu} \rightarrow \nu \tilde{\chi}_1^0$ ) production. Thus, the physically distinct channels, defined by the number of leptons and jets present,<sup>1</sup> typically have multiple sources. Still, a comparison between the rates for the final states so-defined might be quite revealing. For instance, if  $\tilde{\chi}_1^\pm \rightarrow \tilde{\ell}^\pm \tilde{\nu}$  is not kinematically allowed, the  $\tilde{\chi}_1^+ \tilde{\chi}_1^-$  final states are expected to yield more  $1\ell + 2j$  and  $0\ell + 4j$  events than  $2\ell + 0j$  events, whereas  $\tilde{\ell}^+ \tilde{\ell}^-$  events will yield only  $2\ell + 0j$  events. Further, the  $\ell$ 's must be of the same type in this latter case. The effective branching fraction for  $\tilde{\chi}_1^+ \tilde{\chi}_1^- \rightarrow \ell^+ \ell^- + \cancel{E}_T$  with both  $\ell$ 's of the same type is only 1/81. In addition, the  $\ell$ 's in the latter derive from three-body decays of the  $\tilde{\chi}_1^\pm$ , and would be much softer on average than  $\ell$ 's from  $\tilde{\ell}^+ \tilde{\ell}^-$ . Even if this difference is difficult to see directly via distributions, it will lead to higher efficiency for picking up the  $\tilde{\ell}^+ \tilde{\ell}^-$  events.

Based on the above discussion, the following ratios would

<sup>1</sup>The totally invisible final state would be  $[0\ell][0j]$ , and so forth.

appear to be potentially useful.

$$\frac{B(H^0 \rightarrow b\bar{b})B(A^0 \rightarrow [0\ell][0j]) + B(A^0 \rightarrow b\bar{b})B(H^0 \rightarrow [0\ell][0j])}{B(H^0 \rightarrow b\bar{b})B(A^0 \rightarrow \text{SUSY}) + B(A^0 \rightarrow b\bar{b})B(H^0 \rightarrow \text{SUSY})} \quad (8)$$

$$\frac{B(H^0 \rightarrow b\bar{b})B(A^0 \rightarrow [2\ell][0j]) + B(A^0 \rightarrow b\bar{b})B(H^0 \rightarrow [2\ell][0j])}{B(H^0 \rightarrow b\bar{b})B(A^0 \rightarrow \text{SUSY}) + B(A^0 \rightarrow b\bar{b})B(H^0 \rightarrow \text{SUSY})} \quad (9)$$

$$\frac{B(H^0 \rightarrow b\bar{b})B(A^0 \rightarrow [\geq 0\ell][0j]) + B(A^0 \rightarrow b\bar{b})B(H^0 \rightarrow [\geq 0\ell][0j])}{B(H^0 \rightarrow b\bar{b})B(A^0 \rightarrow \text{SUSY}) + B(A^0 \rightarrow b\bar{b})B(H^0 \rightarrow \text{SUSY})} \quad (10)$$

$$\frac{B(H^0 \rightarrow b\bar{b})B(A^0 \rightarrow [0\ell][\geq 1j]) + B(A^0 \rightarrow b\bar{b})B(H^0 \rightarrow [0\ell][\geq 1j])}{B(H^0 \rightarrow b\bar{b})B(A^0 \rightarrow \text{SUSY}) + B(A^0 \rightarrow b\bar{b})B(H^0 \rightarrow \text{SUSY})} \quad (11)$$

$$\frac{B(H^0 \rightarrow b\bar{b})B(A^0 \rightarrow [1\ell][\geq 1j]) + B(A^0 \rightarrow b\bar{b})B(H^0 \rightarrow [1\ell][\geq 1j])}{B(H^0 \rightarrow b\bar{b})B(A^0 \rightarrow \text{SUSY}) + B(A^0 \rightarrow b\bar{b})B(H^0 \rightarrow \text{SUSY})} \quad (12)$$

$$\frac{B(H^+ \rightarrow [1\ell][0j])B(H^- \rightarrow b\bar{t}) + B(H^- \rightarrow [1\ell][0j])B(H^+ \rightarrow t\bar{b})}{B(H^+ \rightarrow \text{SUSY})B(H^- \rightarrow b\bar{t}) + B(H^- \rightarrow \text{SUSY})B(H^+ \rightarrow t\bar{b})} \quad (13)$$

$$\frac{B(H^+ \rightarrow [\geq 1\ell][0j])B(H^- \rightarrow b\bar{t}) + B(H^- \rightarrow [\geq 1\ell][0j])B(H^+ \rightarrow t\bar{b})}{B(H^+ \rightarrow \text{SUSY})B(H^- \rightarrow b\bar{t}) + B(H^- \rightarrow \text{SUSY})B(H^+ \rightarrow t\bar{b})} \quad (14)$$

$$\frac{B(H^+ \rightarrow [0\ell][\geq 1j])B(H^- \rightarrow b\bar{t}) + B(H^- \rightarrow [0\ell][\geq 1j])B(H^+ \rightarrow t\bar{b})}{B(H^+ \rightarrow \text{SUSY})B(H^- \rightarrow b\bar{t}) + B(H^- \rightarrow \text{SUSY})B(H^+ \rightarrow t\bar{b})} \quad (15)$$

Also of interest are ratios of the different numerator terms to one another within the above neutral and charged Higgs boson sets. All the ratios that one can form have the potential to provide important tests of the Higgs decays to the supersymmetric particle pair final states. We find that the ratios of rates of the various SUSY channels can contribute significantly to our ability to discriminate between different GUT scenarios. To illustrate, we follow the same procedure as in Table III. Taking  $m_{A^0} = 349.7 \text{ GeV}$  and  $m_{\tilde{\chi}_1^\pm} = 149.5 \text{ GeV}$ , we assume that the correct scenario is  $D^-$  and compute the  $\Delta\chi^2$  by which the prediction for a given ratio in the other scenarios deviates from the  $D^-$  prediction. Statistics are computed on the basis of the expected  $D^-$  rates. The resulting  $\Delta\chi^2$  values are given in Table IV. Since these ratios are not all statistically independent of one another, we do not sum their  $\Delta\chi_i^2$ 's to obtain an overall discrimination level. However, a rough indication of the level at which any given scenario can be ruled out relative to the  $D^-$  is obtained if we add the largest  $\Delta\chi_i^2$  from the neutral Higgs list and the largest from the charged Higgs list. The weakest discrimination level following this procedure is  $\Delta\chi^2 \sim 15$  in the case of the  $D^+$  scenario. Note that this scenario is highly unlikely on the basis of the earlier  $\sum_i \Delta\chi_i^2$  value listed in Table III. In Table III, the weakest discrimination was that for the  $HS^-$  scenario with  $\sum_i \Delta\chi_i^2 \sim 68$ . We observe from Table IV that the ratio  $B(H^0, A^0 \rightarrow [0\ell][0j])/B(H^0, A^0 \rightarrow [2\ell][0j])$  has  $\Delta\chi_i^2 \sim 928$  for the  $HS^-$  case, which would certainly rule it out.

The above illustrations demonstrate that the ratios of rates for individual SUSY channels correlate strongly with the underlying physics of the different GUT scenarios (light vs. heavy sleptons in particular) and add a powerful component to our ability to determine the correct scenario.

## II. Discussion and Conclusions

Once the Higgs bosons are detected and their masses determined, the relative branching fractions for the decay of a single Higgs boson can be measured by ‘tagging’ (*i.e.* identifying) one member of the  $H^0 A^0$  or  $H^+ H^-$  pair in an all-jet mode, and then looking at the ratios of the numbers of events in differ-

Table IV: We tabulate  $\Delta\chi_i^2$  (relative to the  $D^-$  scenario) for the indicated ratios as a function of scenario, assuming the measured  $m_{A^0}$  and  $m_{\tilde{\chi}_1^\pm}$  values are 349.7 GeV and 149.5 GeV, respectively. The SUSY channels have been resolved into final states involving a restricted number of leptons and jets. Only those ratios with substantial power for discriminating between scenarios are tabulated. The error used in calculating each  $\Delta\chi_i^2$  is the approximate  $1\sigma$  error with which the given ratio could be measured for  $L_{\text{eff}} = 80 \text{ fb}^{-1}$  at  $\sqrt{s} = 1 \text{ TeV}$  assuming that the  $D^-$  scenario is the correct one.

Ratio	D <sup>+</sup>	NS <sup>-</sup>	NS <sup>+</sup>	HS <sup>-</sup>	HS <sup>+</sup>
$\langle H^0, A^0 \rangle$					
$[0\ell][0j]/\text{SUSY}$	3.5	193	3.4	1.4	0.6
$[\geq 0\ell][0j]/\text{SUSY}$	0.4	15.3	6.8	20.9	15.8
$[0\ell][0j]/[2\ell][0j]$	9.6	503	0.1	928	105
$[0\ell][0j]/[\geq 0\ell][0j]$	5.8	41.9	0.03	48.4	24.5
$[0\ell][0j]/[0\ell][\geq 1j]$	1.4	1074	6.4	3.5	2.7
$[0\ell][0j]/[1\ell][\geq 1j]$	0.3	3520	4.3	0	1.4
$H^+$					
$[\geq 1\ell][0j]/\text{SUSY}$	1.0	56.2	75.2	3.4	0.5
$[0\ell][\geq 1j]/\text{SUSY}$	2.1	21.7	33.4	1.3	0
$[\geq 1\ell][0j]/[0\ell][\geq 1j]$	5.2	930	5738	4.0	0.4

ent event classes on the opposing side. In this way, the relative branching ratios of Eqs. (1)-(4), Eqs. (5)-(7), Eqs. (8)-(12), and Eqs. (13)-(11) can be measured with reasonable accuracy whenever parameters are such that the final states in the numerator and denominator both have significant event rate.<sup>2</sup> We find that the measured Higgs masses and relative branching fractions, in combination with direct measurements of the chargino and neutralino masses, will over-constrain and very strongly limit the possible SUSY GUT models.

The specific SUSY GUT models we considered are moderately conservative in that they are characterized by universal boundary conditions. The strategy for checking the consistency of a given GUT hypothesis is straightforward. First, the measured  $A^0$ , neutralino and chargino masses are, in almost all cases, already sufficient to determine the  $m_{1/2}$  and  $\tan\beta$  values required in the given GUT scenario with good precision. The Higgs sector branching fractions can then be predicted and become an important testing ground for the consistency of the proposed GUT hypothesis as well as for testing the MSSM two-doublet Higgs sector structure per se. Typically, a unique model among the six rather similar models is singled out by combining measurements from the Higgs sector with those from conventional SUSY pair production. In short, measurements deriving from pair production of Higgs particles can have a great impact upon our ability to experimentally determine the correct SUSY GUT model.

The above discussion has left aside the fact that for universal soft-scalar masses the measured value of the slepton mass would determine the relative magnitude of  $m_0$  and  $m_{1/2}$ , thereby restricting the possible scenarios (see Table I). How-

<sup>2</sup>In some cases, absolute event rates are so different that they would also provide substantial discrimination between different models, despite the possibly large systematic errors.

ever, if the soft-scalar slepton mass is not the same as the soft-scalar Higgs field masses at the GUT scale, the branching fraction ratios would give the best indication of the relative size of the soft-scalar Higgs mass as compared to  $m_{1/2}$ .

More information regarding the slepton/sneutrino mass scale and additional ability to discriminate between models are both realized by subdividing the SUSY decays of the Higgs bosons for slepton/sneutrino vs. chargino/neutralino decays. Slepton/sneutrino channels essentially only produce leptons in the final state, whereas the jet component is typically larger than the leptonic component for chargino/neutralino decays (other than the totally invisible  $\tilde{\chi}_1^0\tilde{\chi}_1^0$  mode). Thus, we are able to define individual SUSY channels, characterized by a certain number of leptons and/or jets, which display a strong correlation with the slepton/sneutrino decay component. We find that these individual channels have sufficiently large event rates that the ratios of the branching fractions for these channels can typically be determined with reasonable statistical precision. Excellent discrimination between models on this basis is found.

In conclusion, our study shows that not only will detection of Higgs pair production in  $e^+e^-$  or  $\mu^+\mu^-$  collisions (at planned luminosities) be possible for most of the kinematically accessible portion of parameter space in a typical GUT model, but also the detailed rates for and ratios of different neutral and charged Higgs decay final states will very strongly constrain the choice of GUT-scale boundary conditions. In estimating experimental sensitivity for Higgs pair detection and for measuring Higgs masses and branching fractions, we included substantial inefficiencies and all relevant branching fractions. Although we believe that our estimates are relatively conservative, it will be important to re-visit this analysis using a full Monte Carlo detector simulation.

## REFERENCES

- [1] J.F. Gunion, A. Stange, and S. Willenbrock, "Weakly-Coupled Higgs Bosons", in *Electroweak Symmetry Breaking and New Physics at the TeV Scale*, edited by T.L. Barklow, S. Dawson, H.E. Haber, and J.L. Siegrist (World Scientific, Singapore, 1996).
- [2] J.F. Gunion and J. Kelly, preprint UCD-96-24.